LAWRENCE
LIVERMORE
NATIONAL
LABORATORY

LLNL-CONF-424406

Autoignition behavior of unsaturated hydrocarbons in the low and high temperature regions

M. Mehl, W. J. Pitz, C. K. Westbrook, K. Yasunaga, H. J. Curran

February 23, 2010

WSSCI
Boulder, CO, United States
March 22, 2010 through March 23, 2010

Disclaimer

This document was prepared as an account of work sponsored by an agency of the United States government. Neither the United States government nor Lawrence Livermore National Security, LLC, nor any of their employees makes any warranty, expressed or implied, or assumes any legal liability or responsibility for the accuracy, completeness, or usefulness of any information, apparatus, product, or process disclosed, or represents that its use would not infringe privately owned rights. Reference herein to any specific commercial product, process, or service by trade name, trademark, manufacturer, or otherwise does not necessarily constitute or imply its endorsement, recommendation, or favoring by the United States government or Lawrence Livermore National Security, LLC. The views and opinions of authors expressed herein do not necessarily state or reflect those of the United States government or Lawrence Livermore National Security, LLC, and shall not be used for advertising or product endorsement purposes.

Autoignition behavior of unsaturated hydrocarbons in the low and high temperature regions

Marco MEHL, William J. PITZ, Charles K. WESTBROOK,

Lawrence Livermore National Laboratory, Livermore, CA 94550 - USA

Kenji YASUNAGA, Henry J. CURRAN

National University of Ireland, Galway - Ireland

Abstract

In this work, numerical and experimental techniques are used to investigate the effect of the position of the double bond on the ignition properties of pentene and hexene linear isomers. A wide-range kinetic model for the oxidation of C_5-C_6 linear alkenes has been developed. Literature rapid compression machine data were used to validate the model at low temperatures and new shock tube experiments were performed in order to assess the behavior of the considered alkenes in the high temperature region.

Some interesting inversions in the relative reactivity of the isomers were detected. The model successfully reproduced the measured behavior and allowed to explain the reason of these reactivity changes. The information gathered will be applied to the development of the kinetic mechanisms of larger unsaturated surrogate components.

1. Introduction

Computational fluid dynamics codes with chemical kinetic models are consolidated tools for the investigation of engine performance and the development of more efficient combustion strategies. The increasing power of modern computer makes virtually possible to couple the detailed fluid dynamic modeling with a detailed description of the combustion kinetics [1-3]. For this reason, the development of such models represents a valuable resource in facing the new demands of energy industry.

Nevertheless, the modeling of real fuel represents a tough challenge. Real fuels are complex mixture of hundreds of compounds whose exact composition cannot be easily determined. Even knowing the exact formulation of such blends, modeling the huge number of species involved in their oxidation still would be far beyond the present capabilities. For this reason simpler surrogates are generally adopted.

For a long time n-heptane and iso-octane have been used as an approximation of real fuels in most of the experimental and numerical investigations of gasoline and diesel fueled engines. The evolution of oil industry is pushing towards new kinds of fuels whose compositions are more and more different from conventional fuels. New kind of feedstock and the spreading of biofuels are shaping a new generation of fuel requiring the development of sophisticated kinetics models to account for more varied compositions [4-5].

Alkenes are one of the fuel components of interest. Alkenes are formed during the refining of crude oil to gasoline by cracking the heavier fractions. Light alkenes (C4-C5) are generally converted into valuable saturated branched components by alkylation processes. However, both American and European gasolines contain a significant amount of these unsaturated species [6].

Their presence has both advantages and drawbacks: short chain alkenes have a much higher knock resistance than their saturated homologues [7]; on the other hand, at high concentrations they can alter the stability of the fuel and promote the formations of gums, detrimental for engine injectors.

One more reason for interest in this class of compounds is the fact that biodiesels are constituted by most part of unsaturated fatty acid esters. The number of double bonds along the linear carbon chain attached to the ester group affects the cetane number of the fuel and, as of today, very few kinetic models and experimental works have investigated the reactivity of unsaturated bio esters.

In this paper, the role of the double bond on ignition properties has been investigated by means of modeling and experimental techniques. A wide-range kinetic model for the oxidation of C5-C6 linear alkenes has been validated by comparison with literature experimental data. New shock tube experiments were performed in order to assess the behavior of the fuels of interest in the high temperature region. The effects of the position of the double bond into the alkyl chain are discussed with the help of calculations.

2. Previous works

Contrary to alkanes, the oxidative behavior of alkenes has been relatively little investigated.

The effect of olefin addition on n-heptane cool flames combustion of different olefins was already noticed in 1971 by Tipper and Titehard [8]. Reviewing work on pentenes, the first systematic study of the low temperature combustion of pentene isomers was carried out by Hughes and Prodhan [9], who investigated the development of cool flames by 1- and 2-pentene in a closed vessel. A study on the low temperature oxidation products of 1 and 2-pentene diluted in a H2/O2 mixture was carried out by Baldwin et al. [10] in 1980. Sixteen years later, Prabhu et al. [11] analyzed the oxidation of 1-pentene in a flow reactor at 6 atm from 600 – 800K at 0.4

equivalence ratio, providing the first speciation data of neat 1-pentene. More recently Minetti et al. compared the ignition behavior of pentane and 1-pentene in a rapid compression machine (RCM) device [12].

Reviewing work on hexenes, Yahyaoui et al [13-14] provided speciation data on the oxidative behavior of 1-hexene in a jet stirred reactor and ignition delay times in a shock tube. The first systematic study on the effect of the position of the double bond in hexene isomers was provided by Vanhove et al. [15], who determined the ignition behavior the three hexene isomers in a rapid compression machine at different pressure.

Though the oxidation of alkenes represents an important submechanism in the combustion of higher alkanes, no low temperature mechanisms for this class of compounds were available until recently. The first studies including a low temperature branching mechanism for alkenes were carried out by Mehl et al. [16] in a joint collaboration between Milano and LLNL and by the Combustion group in Nancy [17-18].

When comparing the reactivity of the different alkene isomers, the most extensive set of data is the one produced by Vanhove et al. [15]. In this set of experiments is evident how the length of the saturated carbon chain determines the autoignition propensity of alkenes in the low temperature region. Long saturated carbon chains allow the alkyl peroxy isomerization process necessary to sustain a low temperature branching. The set of experiments provided by Vanhove is limited to temperatures lower than 850K. Mehl et al. [16] computations predicted that at higher temperature the reactivity scale of the three isomers of hexene significantly changes. Unfortunately no experimental information was available to validate this statement. In this work the autoignition tendency of the pentene and hexene linear isomers was systematically investigated in both the low and the high temperature region, with data up to 1700K.

3. Experimental

Experiments were carried out in a high pressure and low pressure shock tube. The high pressure shock tube has a stainless steel tube of overall length of 8.76 m, with an internal diameter of 6.3 cm. A double-diaphragm section divides the shock tube into a 3 m long driver section and a 5.73 m test section. Polyester films were used as diaphragms in all experiments, and shock waves were fired by self-rupture of diaphragms. The driver gas used was helium (99.99 % pure; BOC). The operational pressure limit of the shock tube is approximately 60 bar. The diagnostic system involves four pressure transducers. The velocity of the incident shock wave is measured at three locations and is then extrapolated to the end-plate. The pressure at the end wall was monitored by a pressure transducer (PCB, 113A24). The ignition delay time was defined as the maximum rate of rise of the pressure signal.

The low pressure shock tube has a stainless steel tube with a test section measuring 6.22 m in length, with an internal diameter of 10.24 cm, and a barrel-shaped driver section measuring 53 cm in length. The two sections were separated by polycarbonate diaphragm, which bursts when forced into contact with a cross-shaped cutter due to the pressure differential between the high pressure driver section and the low pressure test section. The driver gas used was helium (99.99 % pure; BOC). The diagnostic system involves four pressure transducers. The velocity of the incident shock wave is measured at three locations and is then extrapolated to the end-plate.

The pressure at the end wall was monitored by a pressure transducer (Kistler, 603B). Light emission at 431 nm was detected through a fused silica windows embedded in the end-plate using a photodetector (Thorlabs Inc. PDA55-EC) and a narrow band-pass filter centered at 430 nm with a full-width half-maximum of 10 nm. The ignition delay time was defined as the maximum rate of rise of the emission signal.

The 1-pentene (99.5 % pure) was supplied by TCI, and trans-2-pentene (99 % pure), 1-hexene (99 % pure), trans-2-hexene(97 % pure) and trans-3-hexene (99 % pure) were done by Sigma-Aldrich and de-gassed through a series of freeze-thaw-pump cycles, after which no more gas was observed to escape on thawing the solid. The oxygen (99.5% and 99.999 % pure), argon (99.999% pure) and nitrogen (99.5% pure) were supplied by BOC. Mixtures were made up using the method of partial pressures and their compositions are given in Appendix A.

Pentene isomers experiments have been performed at equivalence ratios of 0.5, 1 and 2 and at ranges of pressures 0.93-1.16 atm and 7.8-10.8 atm over a range of temperatures from 993 to 1770 K. Hexene isomers experiments have been done at an equivalence ration of 1 at a ranges of pressures 8.5-12.1 atm over a range of temperatures from 990 to 1460 K.

The incident shock velocity at the endwall was used to calculate the temperature and pressure of the mixtures behind the reflected shock wave using the equilibrium program Gaseq [19]. The thermodynamic data needed for the program of the pentene and hexene isomers were calculated using the THERM program of Ritter and Bozzelli [20], based on group additivity methods developed by Benson [21]. These data are in agreement with estimates in the NIST WebBook [22].

4. Modeling Approach

A previous modeling activity carried out in collaboration with the combustion group in Milano already investigated the oxidation of hexenes in a wide range of conditions. The kinetic model developed at that time was based on the Milano's base chemistry and their lumped species approach. A limited amount of experimental data was available at high temperature for all the three isomers so the direct comparison was mainly focused in the low temperature region where

more data was available. A more careful analysis of the high temperature region is here presented in the framework of the LLNL fully detailed approach.

The model here presented is a development of the kinetic mechanism compiled collaboratively at LLNL and the National University of Ireland, Galway. The mechanism is based on a C_1-C_4 detailed core detailed mechanism which has been recently improved by Curran and coworkers [23-24]. On the top of this model, different modules have been built accounting for different cases of compounds: linear, branched and aromatic hydrocarbons.

Low Temperature Reactivity

The low temperature oxidation of the linear alkenes is dominated by the chemistry of the allyl radical. Firstly, the weak allylic C-H bond makes the abstraction reaction on this site extremely favored. Depending on the position of the double bond, and the length of the residual saturated chain, low temperature reactions may occur. The availability of a saturated chain with a least three carbons makes possible facile isomerization of the hydroperoxyl radicals (ROO) to the peroxyalkyl (QOOH) radicals though a six-membered transition state. This reaction opens the way to the formation of ketohydroperoxides and low temperature branching production of OH radicals. For this reason 1-alkenes have the highest reactivity among the large n-alkene isomers.

This behavior has been experimentally detected in several occasions, including by Hughes and Prodhan [9] in the early '70s and by Vanhove et al. [15] in more recent times. The low temperature branching pathway typical of the alkanes competes with the radical addition on the double bond. The formation of the adduct (HOR.H) has a negligible activation energy and is extremely favored at low temperature. The resulting radical can undergo O_2 addition and, later, decompose via Waddington mechanism.

Secondly, allyl radicals are resonantly stabilized and relatively unreactive compared to alkyl radicals. Due to their unreactivity, they accumulate in large concentrations making reaction with HO_2 radicals important. This reaction forms reactive OH radicals and alkenoxy radicals. The later readily undergoes beta decompositions to smaller oxygenated structures.

High Temperature Reactivity

When the temperature is higher than 900K, the low temperature pathways become less effective. The addition of O2 on alkenyl radicals is no longer favored and the β-decomposition of alkenyl radicals takes over. The presence of double bonds inhibits some cleavages and favors the formation of resonantly stabilized fragments. When the temperature further increases, unimolecular alkene decomposition (initiation) becomes competitive with H-atom abstractions and the composition of the radical pool is totally determined by the relative strength of the C-C bonds along the fuel molecule. Fig. 1 summarizes the different mechanisms that take place across the increasing temperature ranges.

The transition from a low to high temperature oxidation mechanisms is responsible for the unexpected inversions in reactivity of the isomers with increasing temperature discussed here, as will be presented in the next paragraphs.

5. Results

The low temperature data presented here were collected by Vanhove et al [15] for the hexane isomers and Minetti et al. [9] for 1-pentene in the Lille rapid compression machine facility. All the high temperature ignition delay times here presented were recently collected in Galway using the two shock tube described in the experimental section and have not been report previously.

All the simulations were performed using the commercial CHEMKIN PRO code and the Milano's DSMOKE code.

Since the low temperature autoignition of alkenes typically require long delays, rapid compression machine (RCM) simulations have to account for the heat loss affecting the experimental measurements. Non reactive pressure traces were used to calibrate the heat loss coefficient. Since all the RCM data were collected in the same device at similar conditions, the same parameters have been adopted for all the simulations. This approximation affected mostly the slowest ignition delay times, while the effect on most of other conditions of interest can be reasonably assumed to be negligible for the purpose of this discussion. Shock tube data were simulated assuming the conditions behind the shock wave assuming adiabatic, constant volume conditions.

Hexene isomers

Figure 2 shows the comparisons between calculated and measured ignition delay times at about 10 atm over a wide range of temperature. The oxidizer is simulated air and the equivalence ratio equal to 1.

The model correctly reproduces the ignition delay times over the whole range of conditions for all the three isomers. The position of the double bond determines the effectiveness of the low temperature branching mechanism. According to the experimental data, 1 and 2-hexenes show some cool flame formation, 3-hexene doesn't have this possibility. The model successfully reproduces this behavior. A reaction pathway analysis performed by the authors showed that in the temperature range comprised between 650K and 800K the main consumption pathways of 1 and 2-hexene are triggered by the low temperature branching. Both the two isomers can form hex-1-en-3-yl radicals by the abstraction of secondary or primary allylic hydrogens. Hex-1-en-3-yl can undergo O2 addition and start the pathway leading to ketohydroperoxides.

In the case of 3-hexene the attack on to the double bond and the following decomposition to small oxygenates are the main oxidation routes. The most energetically favored abstractions are on the secondary allylic hydrogens. The resulting hex-2-en-4-yl radicals hardly undergo the same pathway previously described because of the lack of secondary hydrogens available for the six member isomerization of the ROO structures. Direct elimination of HO_2 and diolefin formation is then preferred. Further details on this mechanism can be found in Mehl et al [16].

When the temperature increases, decomposition reactions and HO_2 chemistry take over the degenerative branching path and the relative reactivity of the three fuels changes.

1-hexene, the fastest reacting isomer of the three isomers at low temperature conditions, appears to be the slowest reacting isomer for temperatures above 1400K while 2-hexene becomes the fastest reacting. Figure 2 shows in better detail the high temperature region here studied. The reversed reactivity shown by the experiments can be explained by the population of the radical pool generated by the different isomers. When temperature reaches 1000K, the decomposition of the resonantly stabilized hexenyl radicals become the main consumption pathway of the fuel. The hex-1-en-3-yl formed by 1 and 2-hexene forms butadiene and highly reactive ethyl radicals. Hex-2-en-4-yl radical is instead the precursor of the slower methyl radical. When the temperature rises to 1400K, initiation reaction (hexene decomposition) dominates and the position of the double bond dictates the composition of the fragments depending on the weakest C-C bond. 1-hexene forms the slowly reacting allyl and 1-propyl radicals (the last of the two ultimately decomposes to ethylene and methyl), while 2-hexene decomposes to ethyl and but-1-en-3-yl radicals: both of the two fragments stabilize by eliminating H radicals that speed the reactivity. 3-hexene decomposition leads to the formation of butadiene and two methyl radicals, which confer to this fuel a reactivity slightly superior to the one of 1-hexene.

Pentene isomers

Figure 4 shows the calculated ignition delay times of the two pentene isomers here considered: 1 and 2-pentene. The RCM data covering the 650K-850K temperature range were collected between 7 and 9 bar, while the shock tube data at about 10 bar. Unfortunately no RCM data were available for 2-pentene while no high pressure data were collected for 1-pentene. Modeling results suggest that differently from 1-pentene, 2-pentene shows extremely reduced low temperature reactivity. The slower reactivity of 2-pentene is consistent with the findings of Hughes and Prodhan [9]. A reaction pathway analysis showed that the only low temperature reactivity shown by 2-pentene comes from the pent-1-en-3-yl radical formed by the abstraction of the primary allyl hydrogens. Most of the consumption of the fuel still come from the attack on the double bond, similarly to what happen in the case of 3-hexene. When the temperature increases the reactivity of the two isomers tends to become the same.

In order to confirm the validity of the model in the high temperature region some validation at lower pressure was performed. Figure 5 shows the calculated ignition delay times predicted by the model in comparison with experiments carried out in the low pressure shock tube previously described. All the data were collected at atmospheric conditions and fixed fuel concentration.

The model reproduces fairly well the experimental ignition delay times in all the conditions. One discrepancy at the highest equivalence ratio is that the model tends to slightly over predict the activation energy of the ignition delay times. The results are still in line with the experiments and support the validity of the results obtained at higher pressure.

The reason why in the case of pentenes is not possible to observe a clear reactivity inversion as for the hexene isomers, but rather a collapse of the two profiles, is that at high temperature the decomposition of both the two isomers leads to the formation of H radicals. At high temperature

1-pentene readily decomposes to an allyl and an ethyl radical, which forms ethylene and H. 2-pentene leads to methyl and but-1-en-3-yl. The only way this radical can stabilize is through the elimination of an H radical as well. As a result, the high temperature reactivity of the two pentenes is nearly the same.

6. Conclusions

In this paper the autoignition behavior of the pentene and hexene isomers was systematically analyzed by means of experiments and kinetic simulations over a wide range of temperatures. The experiments performed allowed collecting information about the reactivity of this class of compounds in a temperature region scarcely investigated in previous works. Some peculiar inversions in the relative reactivity of the isomers were detected. The model successfully reproduced the measured behavior and provided an interpretative tool for a better understanding of the chemistry of alkenes. The position of the double bond proved to be determining the reactivity of the different isomers not just in the low temperature region, but also at high temperature. The obtained results can be summarized as follows:

1) at low temperature, the reactivity of large alkenes depends on the length of the saturated portions aside the double bond: longer alkyl chains determine shorter ignition delay times, as already discussed in previous works [15-17];
2) at about 1000K, the reactivity is determined by the radicals formed by the β-decompositions of the resonantly stabilized radicals, the most abundant in the system. Fragments leading to the formation of H radicals, such as ethyl radicals, promote the high temperature radical branching;
3) at temperatures above 1400K, the oxidation process is driven by initiation reactions. The presence of the double bond makes the C-C cleavages forming allyl radicals the most

energetically favored. Once again the population of the resulting radical pool determines the reactivity of the fuel. Fragments decomposing to alkenes and H radicals tend to be faster than methyl radicals.

The pieces of information collected in this work provided a validation of the reaction rate rules adopted in the LLNL kinetic model. The same rate constants will be applied for the development of the mechanisms for larger alkenes and unsaturated fatty acid esters contained in biofuels.

7. Acknowledgments

The authors thank program managers Kevin Stork and Gurpreet Singh for their support. This work performed under the auspices of the U.S. Department of Energy by Lawrence Livermore National Laboratory under Contract DE-AC52-07NA27344.

8. References

[1] Z. Liu; R. Chen, Combust. Sci. & Tech. 181 (6) (2009) 828-852.

[2] M. Pasternak, F. Mauss, H. Bensler, SAE 2009-01-0676

[3] C.V. Naik, W.J. Pitz, C.K. Westbrook, M. Sjöberg, J.E.Dec, J. Orme, H.J. Curran, J.M. Simmie; SAE transactions 114 (4) (2005) 1381-1387.

[4] W.J. Pitz, N.P. Cernansky, F.L. Dryer, F.N. Egolfopoulos, J.T. Farrell, D.G. Friend and H. Pitsch SAE 2007-01-0175.

[5] J.T. Farrell, N.P. Cernansky, F.L. Dryer, D.G. Friend, C.A. Hergart, C.K. Law, R.M. McDavid, C.J. Mueller, A.K. Patel and H. Pitsch SAE 2007-01-0201

[6] R.F. Sawyer, Environmental Health Perspectives Supplements 101 (6) (1993) 5-12

[7] M. Mehl, T. Faravelli, F. Giavazzi, E. Ranzi, P. Scorletti, A. Tardani, D. Terna, Energy & Fuels, 20 (2006) 2391-2398

[8] C. F. H. Tipper and A. Titehard, Combust. & Flame 16 (1971) 223-232

[9] R. Hughes and A. S. Prodhan, Combust. & Flame 21 (1973) 297-301

[10] R.R. Baldwin, J.P. Bennett and R.W. Walker, J. Chem. Soc., Faraday Trans. 1, 76 (1980) 2396 - 2412

[11] S. K. Prabhu, R. K. Bhat, , D. L. Miller, N.P. Cernansky Combust. Flame 104 (1996) 377.

[12] R. Minetti, A. Roubaud, E. Therssen, M. Ribaucour and L. R. Sochet, Combust. Flame, 118 (1999) 213–220

[13] M. Yahyaoui, N. Djebaı¨li-Chaumeix, C.-E. Paillard, S. Touchard, R. Fournet, P.A Glaude, F. Battin-Leclerc Proc. Combust. Inst. 30 (2005) 1137–1145.

[14] M. Yahyaoui, N. Djebaïli-Chaumeix, P. Dagaut, C.-E. Paillard , S. Gail Combustion and Flame Volume: 147 (1-2) (2006) 67-78

[15] G. Vanhove, M. Ribaucour, R. Minetti. Proc. Combust. Inst. 30 (2005) 1065-1072.

[16] M. Mehl, G. Vanhove, W. J. Pitz, E. Ranzi, Comb. Flame 155 (2008) 756-772.

[17] S. Touchard, R. Fournet, P.A. Glaude, V. Warth, F. Battin-Leclerc, G. Vanhove, M. Ribaucour and R. Minetti, Proc. Combust. Inst. 30 (1) (2005) 1073-1081.

[18] R. Bounaceur, V. Warth, B. Sirjean, P.A. Glaude, R. Fournet and F. Battin-Leclerc, Proc. Combust. Inst. 32 (1) (2009) 387-394

[19] C. Morley, Gaseq v0.76 http://www.gaseq.co.uk.

[20] E.R. Ritter, J. W. Bozzeli, Int. J. Chem. Kinet. 23 (1991) 767-778.

[21] S. W. Benson, Thermochemical Kinetics, John Wiley & Sons, New York, 1976.

[22] S. E. Stein, R. L. Brown, in: P.J. Linstom, W.G. Mallard (Eds.), Structures and Properties Group Additivity Model in NIST Chemistry WebBook, NIST Standard Reference Database Number 69, June 2005, National Institute of Standards and Technology, Gaitherburg MD, 20899. http://webbook.nist.gov.

[23] Johnson M.V., Goldsborough S.S., Serinyel Z., O'Toole P., Larkin E., O'Malley G., Curran H.J, Energy Fuels 2009, 23, 5886–5898

[24] J. Moc, G. Black, J.M. Simmie, H.J Curran, AIP Conference Proceedings 1148 (2009) 161-4.

Figures

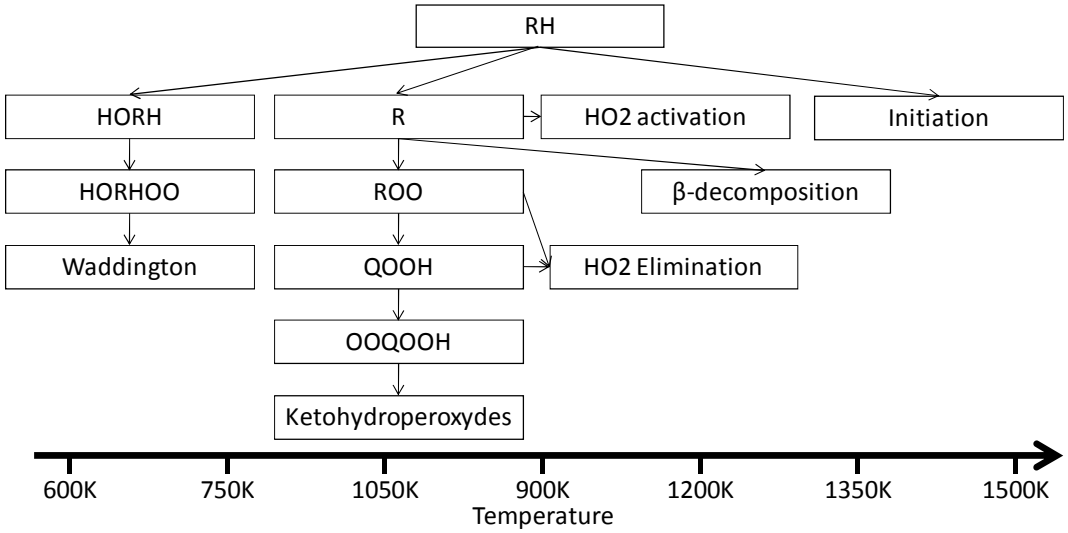

Fig. 1 - Reaction pathways determining the radical pool at different temperatures

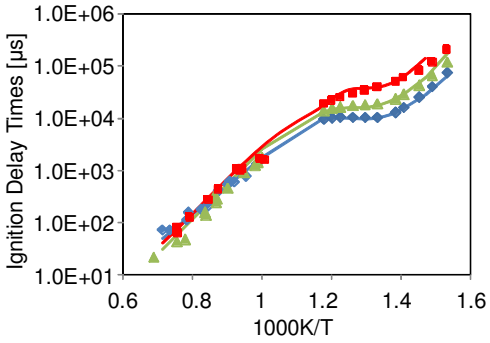

Fig. 2- ignition delay times of hexene isomers temperature in the high pressure shock tube: 10 atm, stoichiometric conditions. 1-hexene (diamonds), 2-hexene (triangles), 3-hexene (squares).

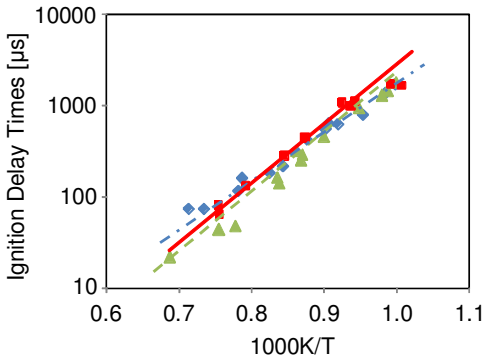

Fig. 3 –ignition delay times of hexene isomers at high temperature: 10 atm, stoichiometric conditions. 1-hexene (Exp: diamonds, Calc: dot-dashed line), 2-hexene (Exp: triangles, Calc: dashed line), 3-hexene (Exp: squares, Calc: solid line).

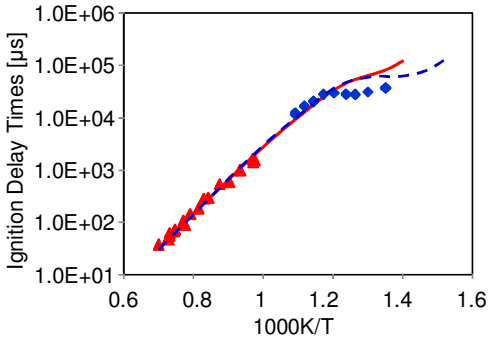

Fig. 4 –ignition delay times of pentene isomers in the high pressure shock tube: 7-10 atm, stoichiometric conditions. 1-pentene (Exp: diamonds, Calc: dashed line) and 2-pentene (Exp: triangles, Calc: solid line).

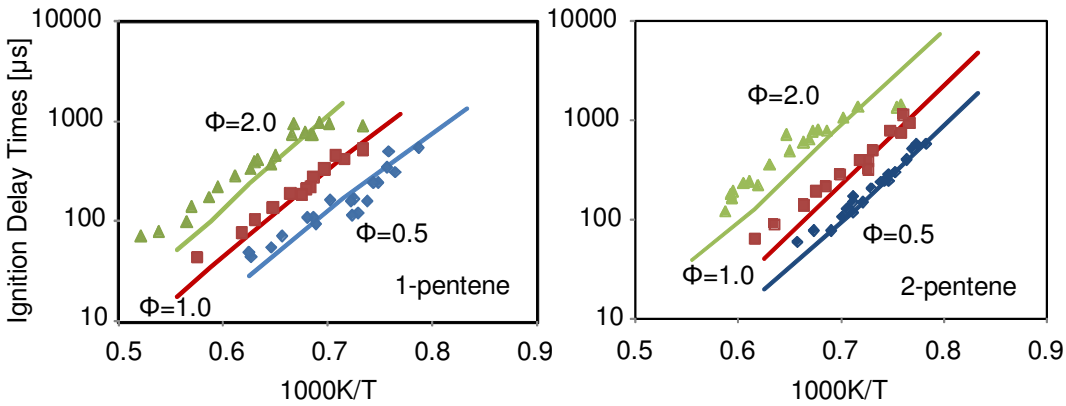

Fig. 5 – Ignition delay times of 1 and 2-pentenes in the low pressure shock tube at different equivalence ratios and atmospheric pressure. Phi = 2 (triangles), 1 (squares), 0.5 (diamonds)

Appendix A

1-pentene Table S-1:

1-pentene; 99.5 % purity from TCI

T_5 [K]	P_5 [atm]	1-Pentene [%]	Oxygen [%]	Ar [%]	Φ (E.R.)	Ignition (pressure) [μs]
1271	0.99	1	15	84	0.5	555.556
1308.1	1.06	1	15	84	0.5	316.667
1318.9	1.08	1	15	84	0.5	511.111
1321.2	1	1	15	84	0.5	355.555
1336.5	0.94	1	15	84	0.5	250
1344.8	1.05	1	15	84	0.5	250
1355	0.87	1	15	84	0.5	161.11
1371.6	0.99	1	15	84	0.5	122.22
1379.3	1.12	1	15	84	0.5	172.222
1382.6	1.02	1	15	84	0.5	116.667
1384	1.04	1	15	84	0.5	161.111
1424	1.06	1	15	84	0.5	166.667
1451.5	1.03	1	15	84	0.5	94.444
1457.1	1.1	1	15	84	0.5	111.111
1469.8	1.078	1	15	84	0.5	111.111
1524.1	1.07	1	15	84	0.5	72.222
1547.3	1.04	1	15	84	0.5	55.555
1596.2	1.02	1	15	84	0.5	44.444
1601.5	1.04	1	15	84	0.5	50

1-pentene Table S-2:

1-pentene; 99.5 % purity from TCI

T_5 [K]	P_5 [atm]	1-Pentene [%]	Oxygen [%]	Ar [%]	Φ (E.R.)	Ignition (pressure) [μs]
1362.8	0.99	1	7.5	91.5	1	533.333
1397.3	1.06	1	7.5	91.5	1	422.222
1413.6	1	1	7.5	91.5	1	466.667
1435.4	1.01	1	7.5	91.5	1	338.889
1457.5	1.03	1	7.5	91.5	1	277.778
1463.2	1.08	1	7.5	91.5	1	222.222
1472	1.02	1	7.5	91.5	1	211.111
1481.5	1.04	1	7.5	91.5	1	188.889
1505.9	1.01	1	7.5	91.5	1	194.444
1544.5	1.01	1	7.5	91.5	1	138.889
1586.8	0.95	1	7.5	91.5	1	105.6
1618.4	1.03	1	7.5	91.5	1	77.778
1738.2	1.03	1	7.5	91.5	1	44.444

1-pentene Table S-3:

1-pentene; 99.5 % purity from TCI

T_5 [K]	P_5 [atm]	1-Pentene [%]	Oxygen [%]	Ar [%]	Φ (E.R.)	Ignition (pressure) [μs]
1637.4	0.95	1	3.75	95.25	2	288.889
1682.9	1.05	1	3.75	95.25	2	222.222
1597.8	1.03	1	3.75	95.25	2	338.889
1363.9	0.83	1	3.75	95.25	2	911.111
1426.1	0.93	1	3.75	95.25	2	944.444
1920.5	1.02	1	3.75	95.25	2	72.222
1859.3	1.04	1	3.75	95.25	2	81.1
1706.9	0.96	1	3.75	95.25	2	177.222
1757.3	0.98	1	3.75	95.25	2	144.444
1771.6	0.98	1	3.75	95.25	2	100
1588.9	1.06	1	3.75	95.25	2	400
1549.1	1.07	1	3.75	95.25	2	377.778
1463	1.01	1	3.75	95.25	2	744.444
1499	1.02	1	3.75	95.25	2	944.444
1446	0.98	1	3.75	95.25	2	972.222
1474.7	1.01	1	3.75	95.25	2	788.888
1503.5	1.03	1	3.75	95.25	2	744.444
1539.3	1.03	1	3.75	95.25	2	466.666
1581.6	1.06	1	3.75	95.25	2	416.667
1459.3	0.96	1	3.75	95.25	2	750

Table S1-3: Ignition delay time data with Ar as the bulk carrier gas measuring the time between the arrival of the reflected shock and the distinct emission rise at 430 nm (the time of the intersection of the linear extrapolation of the emission rise with the pre-ignition emission floor).

2-pentene Table S-4:

2-pentene; 99.0 % purity from aldrich

T_5 [K]	P_5 [atm]	2-Pentene [%]	Oxygen [%]	Ar [%]	Φ (E.R.)	Ignition (emission) [μs]
1278	1.06	1.0	15.0	84.0	0.5	574
1293	0.95	1.0	15.0	84.0	0.5	572
1300	0.99	1.0	15.0	84.0	0.5	513
1310	1.09	1.0	15.0	84.0	0.5	400
1329	1.09	1.0	15.0	84.0	0.5	300
1340	1.05	1.0	15.0	84.0	0.5	283
1340	1.04	1.0	15.0	84.0	0.5	244
1348	1.03	1.0	15.0	84.0	0.5	244
1354	1.05	1.0	15.0	84.0	0.5	239
1371	1.16	1.0	15.0	84.0	0.5	206
1387	1.13	1.0	15.0	84.0	0.5	150
1405	1.12	1.0	15.0	84.0	0.5	172
1406	1.05	1.0	15.0	84.0	0.5	150
1406	1.00	1.0	15.0	84.0	0.5	117
1417	1.08	1.0	15.0	84.0	0.5	128
1427	0.99	1.0	15.0	84.0	0.5	106
1449	1.05	1.0	15.0	84.0	0.5	78
1485	1.01	1.0	15.0	84.0	0.5	78
1521	1.03	1.0	15.0	84.0	0.5	60

2-pentene Table S-5:

2-pentene; 99.0 % purity from aldrich

T_5 [K]	P_5 [atm]	Pentene [%]	Oxygen [%]	Ar [%]	Φ (E.R.)	Ignition (emission) [μs]
1305	1.04	1.0	7.5	91.5	1.0	938
1315	0.94	1.0	7.5	91.5	1.0	1139
1319	0.97	1.0	7.5	91.5	1.0	750
1338	0.97	1.0	7.5	91.5	1.0	783
1368	1.05	1.0	7.5	91.5	1.0	500
1377	1.00	1.0	7.5	91.5	1.0	394
1377	0.95	1.0	7.5	91.5	1.0	320
1393	1.06	1.0	7.5	91.5	1.0	400
1431	0.95	1.0	7.5	91.5	1.0	287
1459	1.00	1.0	7.5	91.5	1.0	217
1481	0.98	1.0	7.5	91.5	1.0	194
1506	0.93	1.0	7.5	91.5	1.0	139
1575	1.02	1.0	7.5	91.5	1.0	89
1623	1.11	1.0	7.5	91.5	1.0	64

2-pentene Table S-6:

2-pentene; 99.0 % purity from aldrich

T_5 [K]	P_5 [atm]	Pentene [%]	Oxygen [%]	Ar [%]	Φ (E.R.)	Ignition (emission) [μs]
1319	0.97	1.0	3.75	95.25	2.0	1444
1326	0.99	1.0	3.75	95.25	2.0	1356
1396	0.98	1.0	3.75	95.25	2.0	1383
1424	0.97	1.0	3.75	95.25	2.0	1061
1457	1.11	1.0	3.75	95.25	2.0	794
1476	1.09	1.0	3.75	95.25	2.0	811
1487	1.01	1.0	3.75	95.25	2.0	778
1494	1.10	1.0	3.75	95.25	2.0	647
1508	1.08	1.0	3.75	95.25	2.0	605
1539	0.98	1.0	3.75	95.25	2.0	494
1547	1.03	1.0	3.75	95.25	2.0	724
1587	1.02	1.0	3.75	95.25	2.0	361
1616	0.98	1.0	3.75	95.25	2.0	222
1638	1.06	1.0	3.75	95.25	2.0	244
1654	1.01	1.0	3.75	95.25	2.0	233
1682	1.07	1.0	3.75	95.25	2.0	194
1685	1.02	1.0	3.75	95.25	2.0	167
1688	1.10	1.0	3.75	95.25	2.0	183
1703	1.00	1.0	3.75	95.25	2.0	122

Table S4-6: Ignition delay time data with Ar as the bulk carrier gas measuring the time between the arrival of the reflected shock and the distinct emission rise at 430 nm (the time of the intersection of the linear extrapolation of the emission rise with the pre-ignition emission floor).

2-Pentene Table S-7:

2-Pentene; 99.0 % purity from aldrich

T_5 [K]	P_5 [atm]	2-Pentene [%]	Oxygen [%]	N_2 [%]	Φ (E.R.)	Ignition (pressure) [μs]
993	10.8	2.8	21.0	76.2	1.0	2120
999	10.0	2.8	21.0	76.2	1.0	1935
1001	10.8	2.8	21.0	76.2	1.0	2260
1042	10.1	2.8	21.0	76.2	1.0	1356
1077	10.5	2.8	21.0	76.2	1.0	774
1115	9.5	2.8	21.0	76.2	1.0	680
1161	9.3	2.8	21.0	76.2	1.0	366
1179	9.6	2.8	21.0	76.2	1.0	350
1201	8.2	2.8	21.0	76.2	1.0	222
1241	10.2	2.8	21.0	76.2	1.0	168
1265	7.8	2.8	21.0	76.2	1.0	100
1275	9.6	2.8	21.0	76.2	1.0	123
1318	9.2	2.8	21.0	76.2	1.0	82
1321	8.9	2.8	21.0	76.2	1.0	74
1346	9.1	2.8	21.0	76.2	1.0	70
1349	9.1	2.8	21.0	76.2	1.0	60
1352	9.1	2.8	21.0	76.2	1.0	51.5
1411	9.9	2.8	21.0	76.2	1.0	40

Table S-7: Ignition delay time data with N_2 as the bulk carrier gas measuring the time between the arrival of the reflected shock and the distinct pressure rise (the time of the intersection of the linear extrapolation of the pressure rise with the pre-ignition pressure floor).

1-hexene Table S-8:

1-hexene; 99.0 % purity from aldrich

T_5 [K]	P_5 [atm]	1-hexene [%]	Oxygen [%]	N_2 [%]	Φ (E.R.)	Ignition (pressure) [μs]
1003	12.1	2.3	20.7	97.0	1.0	1700
1016	11.5	2.3	20.7	97.0	1.0	1380
1049	9.8	2.3	20.7	97.0	1.0	794
1089	11.1	2.3	20.7	97.0	1.0	620
1104	10.4	2.3	20.7	97.0	1.0	640
1110	10.1	2.3	20.7	97.0	1.0	560
1143	10.2	2.3	20.7	97.0	1.0	421
1187	10.0	2.3	20.7	97.0	1.0	214
1213	9.7	2.3	20.7	97.0	1.0	182
1271	9.2	2.3	20.7	97.0	1.0	160
1280	8.7	2.3	20.7	97.0	1.0	115
1363	9.0	2.3	20.7	97.0	1.0	73
1404	9.1	2.3	20.7	97.0	1.0	74

2-hexene Table S-9:

2-hexene; 97.0 % purity from aldrich

T_5 [K]	P_5 [atm]	2-hexene [%]	Oxygen [%]	N_2 [%]	Φ(E.R.)	Ignition (pressure) [μs]
1001	10.8	2.3	20.7	97.0	1.0	1808
1014	11.7	2.3	20.7	97.0	1.0	1460
1021	10.4	2.3	20.7	97.0	1.0	1290
1056	10.2	2.3	20.7	97.0	1.0	938
1112	10.3	2.3	20.7	97.0	1.0	458
1150	10.1	2.3	20.7	97.0	1.0	290
1153	10.1	2.3	20.7	97.0	1.0	250
1162	11.5	2.3	20.7	97.0	1.0	320
1194	10.1	2.3	20.7	97.0	1.0	140
1198	9.8	2.3	20.7	97.0	1.0	162
1287	8.5	2.3	20.7	97.0	1.0	48
1327	9.3	2.3	20.7	97.0	1.0	44
1457	9.9	2.3	20.7	97.0	1.0	22

3-hexene Table S-10:

3-hexene; 99.0 % purity from aldrich

T_5 [K]	P_5 [atm]	3-hexene [%]	Oxygen [%]	N_2 [%]	Φ(E.R.)	Ignition (pressure) [μs]
993	9.1	2.3	20.7	97.0	1.0	1640
1008	11.8	2.3	20.7	97.0	1.0	1712
1061	11.4	2.3	20.7	97.0	1.0	1105
1068	11.1	2.3	20.7	97.0	1.0	985
1081	8.9	2.3	20.7	97.0	1.0	1071
1145	10.0	2.3	20.7	97.0	1.0	442
1183	10.6	2.3	20.7	97.0	1.0	280
1263	10.2	2.3	20.7	97.0	1.0	130
1324	9.6	2.3	20.7	97.0	1.0	64
1326	9.4	2.3	20.7	97.0	1.0	80

Table S8-10: Ignition delay time data with N_2 as the bulk carrier gas measuring the time between the arrival of the reflected shock and the distinct pressure rise (the time of the intersection of the linear extrapolation of the pressure rise with the pre-ignition pressure floor).